

Design, Fabrication, and Characterization of a Dual-Band Electrically Small Meander-line Monopole Antenna for Wireless Communications

C. C. Hsu, H. H. Song*

Department of Electrical and Computer Engineering, University of Colorado, 1420 Austin Bluffs Parkway, Colorado Springs, CO 80918
United States

Abstract A compact, planar, dual-band meander-line monopole antenna that operates in frequency range of 2.400-2.480, 5.150-5.350, and 5.725-5.825 GHz was designed, fabricated, and characterized. Theoretical analysis based on the antenna theory was conducted to obtain the optimum characteristics. A 3-D electromagnetic finite-element solver, high frequency structure simulator (HFSS), was used in antenna simulation. The antenna was fabricated on a Rogers RO4003C substrate with dielectric constant of 3.38 and loss-tangent of 0.002 at 10 GHz and thickness of 0.813 mm. In 2.400-2.480 band, gain of 1.6 dBi and -10 dB frequency bandwidth of 11% were measured. In 5.150-5.350 and 5.725-5.825 bands, gain of 4.3 and 3.9 dBi with 1.14 GHz -10 dB bandwidth were measured. Omnidirectional radiation pattern was obtained for 2.400-2.480 band and double end-fire patterns were observed for 5.150-5.350 and 5.725-5.825 bands. The proposed antenna can be potentially used for portable wireless communication applications.

Keywords Meander Line Antenna, Electrically Small Antenna

1. Introduction

Compact dual band antennas are required for various applications including wireless local area network (WLAN). Recent WLAN communication systems support 2.4/5.0 GHz band such as IEEE 802.11a/b/g/n standard. The 2.4/5.0 GHz band utilizes frequency ranges of 2.400-2.480, 5.150-5.350, and 5.725-5.825 GHz in US. In order to support the increasing need for compact antennas for WLAN communication systems, an electrically small antenna (ESA) has been a subject of great interest [1-4]. In the past decade, portable communication devices have provided an opportunity of using electrically small antennas (ESAs) with highly integrated RF circuit design.

One of the promising ESA structures is the meander-line configuration. It is compact in size and provides wide bandwidth suitable for dual-band operation. Studies on meander-line ESAs were reported. A 700 MHz single-band meander-line ESA was investigated for RFID-tags applications [5]. In this work, the high permittivity substrate and the meander-line configuration improved the inherent deficiencies of low radiation efficiency and low gain of the ESAs.

Studies on the 2.4 GHz printed meander-line antennas were reported for WLAN applications [6]-[7]. Dual-band meander-line ESAs for 1.4/2.4 and 2.4/5.0 GHz bands were reported for GSM/DCS, Bluetooth, and WLAN applications [8]-[11]. However, there still is a need for a meander-line antenna that can provide wider frequency bandwidth for 5.0 GHz band.

In this paper, we propose a compact, dual-band meander-line ESA for WLAN applications. The proposed antenna consists of two meander-line sections, a conducting strip [12]-[13], and a micro-strip matching network. The antenna port impedance is designed to match a 50 Ω coaxial cable. For bandwidth increase in 5 GHz band, the conducting strip is applied within section space of the second meander-line section. By adjusting the dimensions of the second meander-line section and the conducting strip, the proposed antenna can provide the frequency bandwidth for a return-loss less than -10-dB is 11% and 1.14 GHz for 2.4 GHz and 5 GHz band, respectively. Compared to the previously reported results, the proposed antenna provides a particularly better coverage of frequency bandwidth for 5.0 GHz band. The antenna design procedures, simulation and measurement results for return-loss, far-field radiation patterns, and antenna gain are presented.

* Corresponding author:

hsong@uccs.edu (H. H. Song)

Published online at <http://journal.sapub.org/ijea>

Copyright © 2013 Scientific & Academic Publishing. All Rights Reserved

2. Characteristics of an ESA and a Meander-line Section

The ESAs have fundamental limitations to their frequency bandwidth. Wheeler investigated this limitation and indicated that the maximum dimension of an ESA needs to be less than $\lambda/2\pi$ as shown in (1)[1]. In ESAs, higher antenna Q (resonance quality factor) introduces narrower frequency bandwidth. In order to obtain maximum bandwidth, another inherent characteristic that needs to be considered is the minimum Q value. The minimum Q of the ESAs in free space and the gain can be expressed as (2) and (3), respectively [4], [2]. In (3), k is the wavenumber in free space in radians/meter and a is the maximum radius of enclosing sphere of the antenna in meter. The approximate impedance bandwidth in terms of Q is given by (4)[3]. Here S is the VSWR and BW is the normalized bandwidth.

$$ka < 1 \quad (1)$$

$$Q = \frac{1}{k^3 a^3} + \frac{1}{ka} \quad (2)$$

$$G = (ka)^2 + 2(ka) \quad (3)$$

$$BW = \frac{S-1}{Q\sqrt{S}} \quad (4)$$

According to the transmission line theory, a meander-line section shown in Figure 1 can be characterized as a short-circuited transmission line. The proposed antenna is shown in Figure 2. Since no ground plane is underneath meander-line section as shown in Figure 2, it acts as a short-circuited coplanar strip (CPS) structure. In order to obtain the characteristic impedance of a meander-line section printed on a dielectric substrate (quasi-TEM mode), a study on the effective dielectric constant for coplanar waveguide (CPW) was reported (5)[14]. Here $k = b/a$, $k_1 = \sinh(\pi a/2h)/\sinh(\pi b/2h)$, and K is the complete elliptic integral of the first kind, and $k' = \sqrt{1-k^2}$. The approximation for the function K/K' can be expressed as (6)[15] and the characteristic impedance of CPS is shown in (7)[16]. Here $\epsilon_{r_{eff}}$ is given by (5). Assuming the CPS on a dielectric substrate is lossless, the input impedance of a meander-line section on a dielectric substrate is equal to a short-circuited transmission line on a dielectric substrate; the input impedance is given by (8)[17]. Here $\beta = k_o \sqrt{\epsilon_{r_{eff}}}$ is

phase constant of quasi-TEM mode in rad/m, and l is the length of meander-line section in meter. If $\tan(\beta l) \geq 0$, the self-inductance of each meander-line section is given by (9)[17]. This inductive property compensates negative radiation reactance of an antenna of length less than a quarter-wavelength, as shown in Figure 3 [18].

$$\epsilon_{r_{eff}} = 1 + \frac{\epsilon_r}{2} \times \frac{K(k)}{K(k')} \times \frac{K(k_1)}{K(k_1')} \quad (5)$$

$$\frac{K(k)}{K(k')} \approx \begin{cases} \pi / \ln \left[2 \frac{(1+\sqrt{k})}{(1-\sqrt{k})} \right] & \text{for } 1 \leq \frac{K}{K'} \leq \infty \text{ and } 0 \leq k \leq \frac{1}{\sqrt{2}} \\ \frac{1}{\pi} \ln \left[2 \frac{(1+\sqrt{k})}{(1-\sqrt{k})} \right] & \text{for } 0 \leq \frac{K}{K'} \leq 1 \text{ and } \frac{1}{\sqrt{2}} \leq k \leq 1 \end{cases} \quad (6)$$

$$Z_o = \frac{120\pi}{\sqrt{\epsilon_{r_{eff}}}} \times \frac{K(k)}{K(k')} \quad (7)$$

$$Z_{in} = jZ_o \tan(\beta l) \quad (8)$$

$$j\omega L = Z_{in} = jZ_o \tan(\beta l) \quad (9)$$

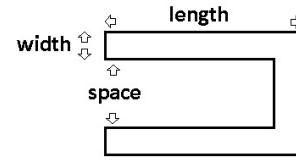


Figure 1. Geometry of a meander-line section

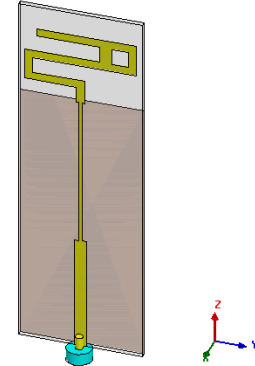


Figure 2. HFSS 3D simulation model of the proposed meander-line monopole antenna. (Substrate: $60 \times 20 \times 0.813$ mm³)

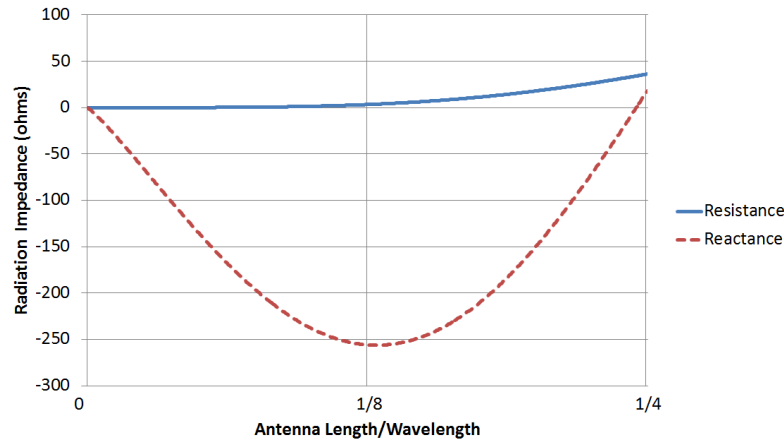


Figure 3. Radiation impedance of a finite length monopole antenna in free space with the resonant frequency of 2.45 GHz and the wire radius of 10^{-6} m

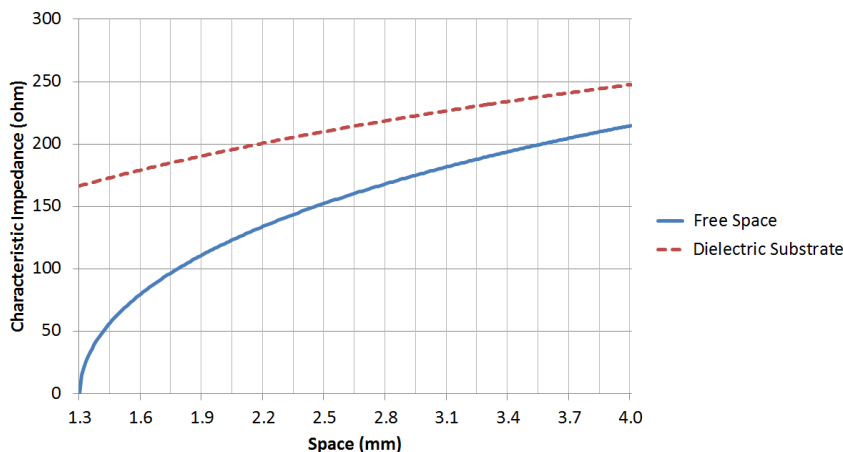


Figure 4. Characteristic impedance of a meander line section with resonant frequency of 2.45 GHz. (Free space: wire radius of 1.3 mm. Substrate: strip line width of 1.3 mm, relative dielectric constant, ϵ_r , of 3.55, and dielectric thickness of 0.813 mm)

Figure 4 is a plot of the characteristic impedance of a lossless meander line section. Given the same conditions, a meander-line section, on a dielectric substrate, has higher characteristic impedance than one within the free space. This indicates that the size of a meander-line section on a dielectric substrate needs to be less than the one within the free space.

3. Simulated Results and Measurement

A close view of the meander line antenna section is shown in Figure 5. Figure 6 shows the S_{11} curve with 'c' dimension variation for fixed values of $a=1.3$ mm and $b=1.3$ mm. Figure 7 describes the S_{11} response with 'a' dimension variation for fixed values of $c=6.5$ mm and $b=1.3$ mm. The optimized dimensions obtained from the 3-D simulation model of the proposed antenna are indicated in Table 1. Simulated gains of the proposed antenna in 2.4GHz (vertical orientation) and 5.0 GHz (horizontally lateral orientation) bands are shown in Figures 8 and 9, respectively.

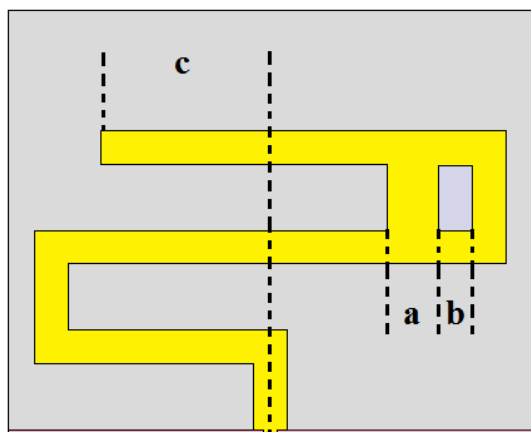


Figure 5. Close view of the meander line antenna section of the proposed antenna

The interference of the surface current on the feeding cable of the ESA was a main concern during the

measurements. This interference will cause undesired radiation. In order to investigate the effects of the surface current on the feeding cable, S_{11} was measured with and without ferrite core which is illustrated in Figure 10. The measurement result indicates that the surface current affects S_{11} dramatically in 2.4 GHz band. Antenna gains of the proposed antenna at three different resonant frequencies are indicated in Table 2. Due to fabrication errors, the measured resonant frequencies of the proposed antenna are shifted approximately 200 MHz higher than the simulated results. The simulated and measured radiation patterns at three different resonant frequencies are illustrated as Figures 11-13. The fabricated dual-band meander-line monopole antenna is shown in Figure 14.

Table 1. Optimized dimensions obtained from the 3-D simulation model of the proposed antenna

Substrate	Width (mm)	20
	Length (mm)	60
	Thickness (mm)	0.813
1 st transformer	Width (mm)	1.9
	Length (mm)	19
2 nd transformer	Width (mm)	0.5
	Length (mm)	25
Strip	Width 'a' (mm)	1.95
	Length (mm)	2.5
1 st Meander-line section	Width (mm)	1.3
	Length (mm)	9
	Space (mm)	2.5
2 nd Meander-line section	Width (mm)	1.3
	Length (mm)	9
	Space (mm)	2.5
	b (mm)	1.3
	c (mm)	6.5

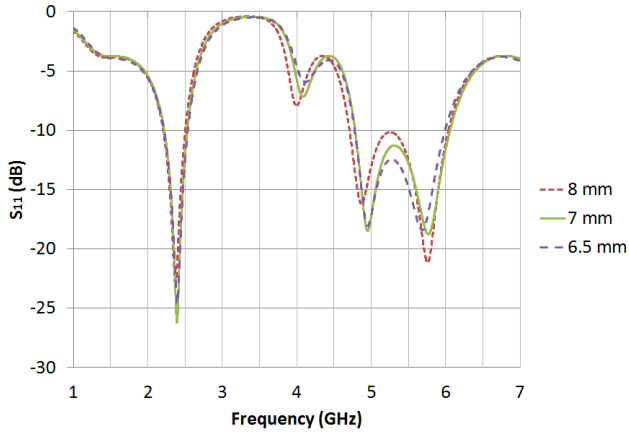


Figure 6. The S₁₁ response of the proposed antenna with 'c' dimension variation for fixed values of a=1.3 mm and b=1.3 mm

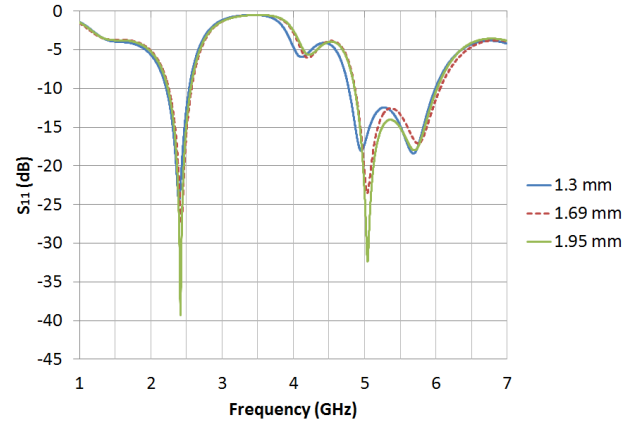


Figure 7. The S₁₁ response of the proposed antenna with 'a' dimension variation for fixed values of c=6.5 mm and b=1.3 mm

Table 2. Antenna gains of the proposed antenna at three different resonant frequencies

Frequency (GHz)	Orientation	Gain (dBi)	
		Simulation	Measurement
2.540	Vertical	1.633	1.615
5.270	Horizontally lateral	4.920	4.285
5.977	Horizontally lateral	4.425	3.885

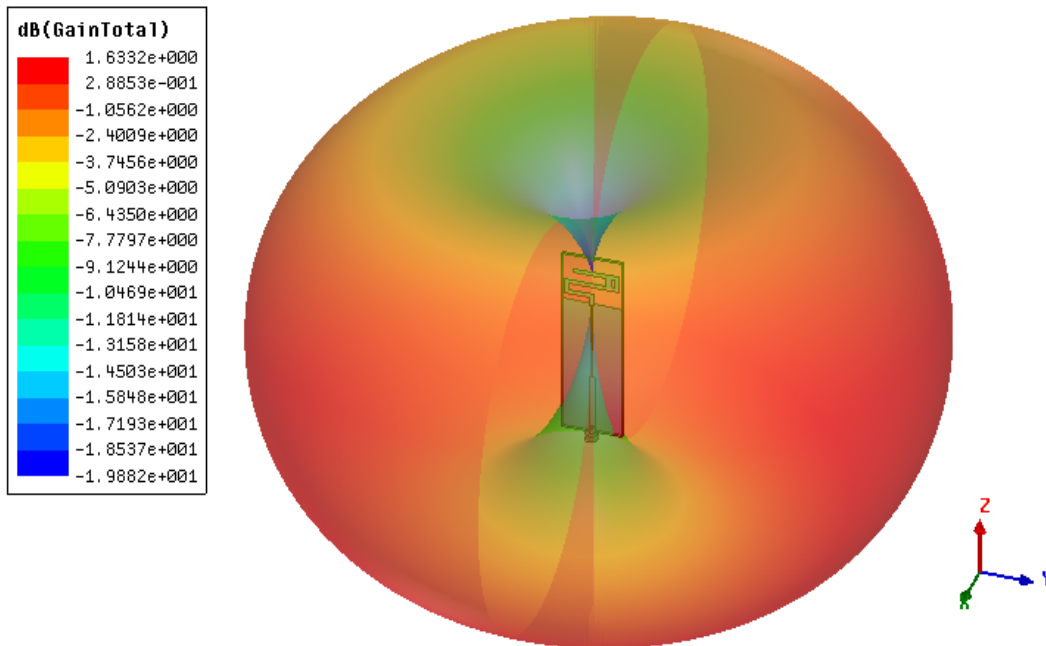
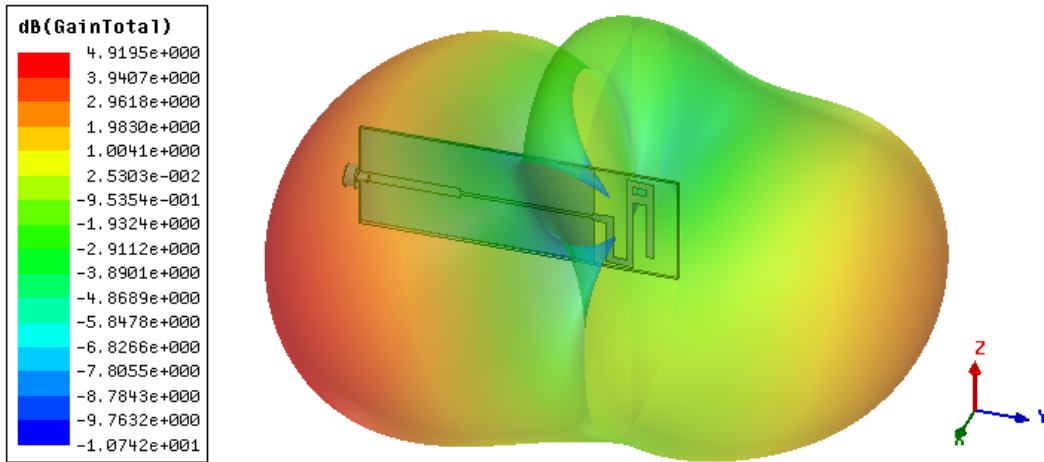
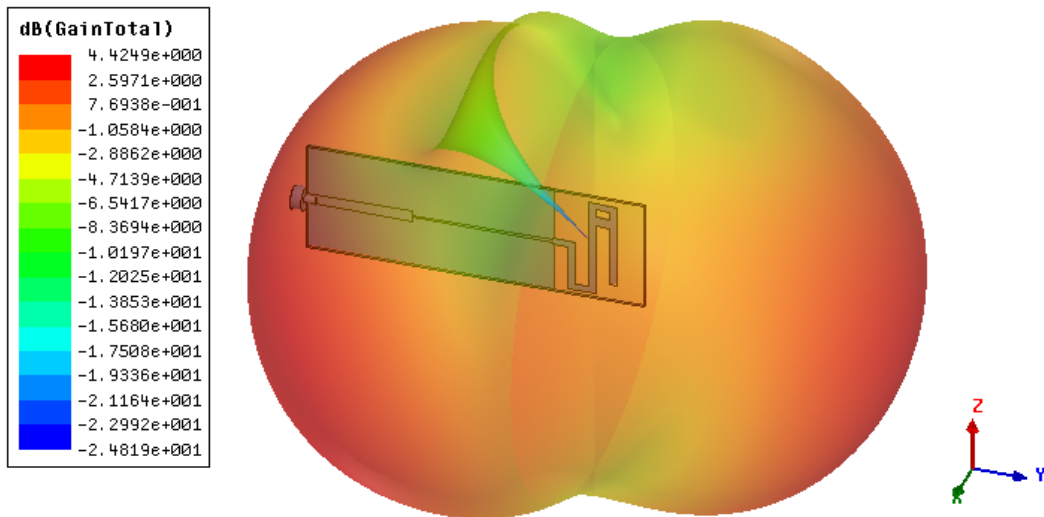


Figure 8. Simulated gain of the proposed antenna at 2.45 GHz (vertical orientation)



(a) 5.026 GHz



(b) 5.761 GHz

Figure 9. Simulated gains of the proposed antenna in 5.0 GHz band (horizontally lateral orientation)

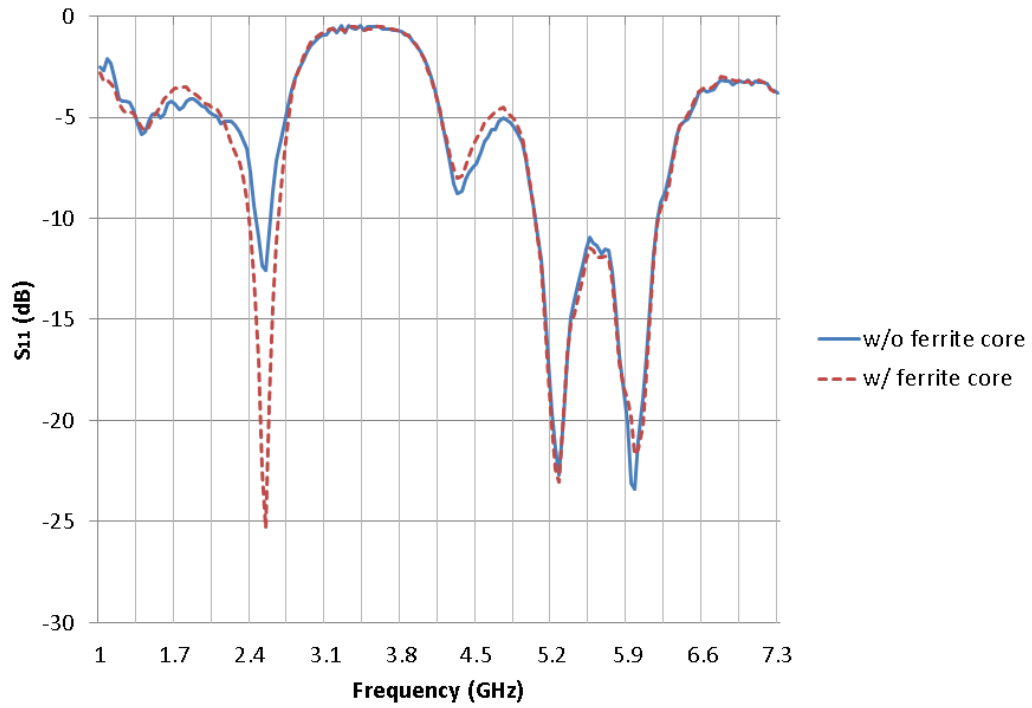


Figure 10. Measured S_{11} curve of the proposed antenna with and without the ferrite core

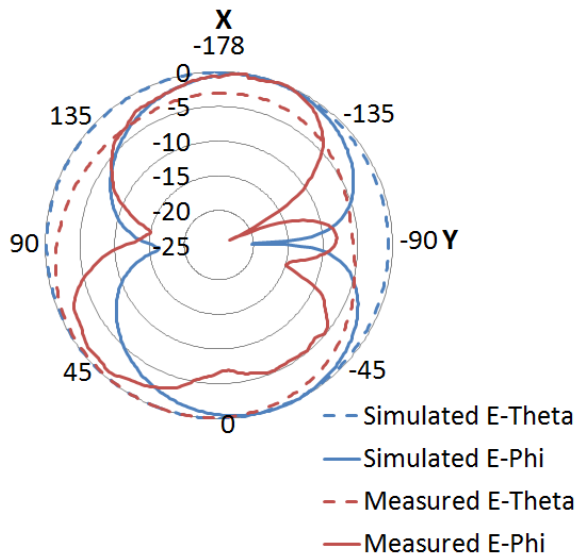


Figure 11. Simulated and measured radiation patterns at 2.54 GHz on vertical orientation

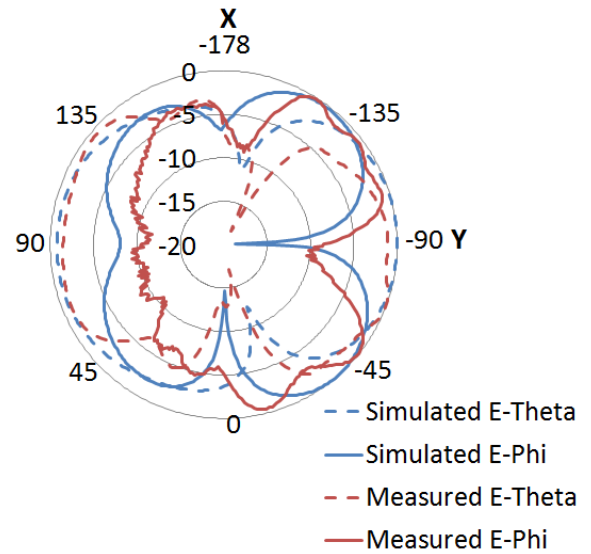


Figure 12. Simulated and measured radiation patterns at 5.27 GHz on horizontally lateral orientation

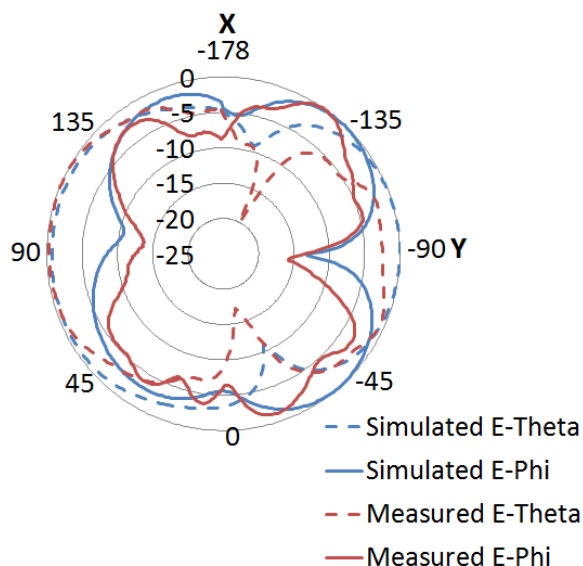


Figure 13. Simulated and measured radiation patterns at 5.977 GHz on horizontally lateral orientation

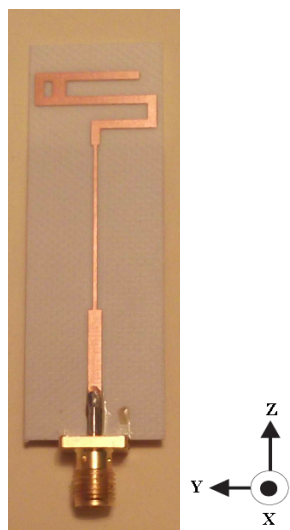


Figure 14. Fabricated dual-band meander-line monopole antenna

4. Summaries and Conclusions

In this paper, a design, fabrication, and characterization of a planar dual-band meander-line monopole antenna are presented. The proposed antenna is compact in size, $60 \times 20 \times 0.813 \text{ mm}^3$, and operates in dual band, 2.4/5.0 GHz, to support WLAN systems. The measured resonant frequencies were within 200 MHz difference compared to the simulated results. The proposed antenna showed 1.6 dBi measured gain and 11% -10-dB frequency bandwidth in 2.4 GHz band in a vertical orientation. In 5.150-5.350 and 5.725-5.825 bands, measured gain of 4.3 and 3.9 dBi were obtained with 1.14 GHz -10-dB frequency bandwidth in a horizontally lateral orientation. An omnidirectional pattern was obtained in 2.4 GHz band and a double end-fire pattern was obtained in the 5.0 GHz band. The proposed antenna can be potentially used for portable WLAN communication devices.

REFERENCES

- [1] H. A. Wheeler, "Fundamental Limitations of Small Antennas," *Proceeding of the I.R.E.*, vol. 35, no. 12, pp. 1479-1484, December 1947.
- [2] R. F. Harrington, "Effect of Antenna Size on Gain, Bandwidth, and Efficiency," *Journal of Research of the National Bureau of Standards-D. Radio Propagation*, vol. 64D, no. 1, pp. 1-12, January-February 1960.
- [3] A. D. Yaghjian and S. R. Best, "Impedance, Bandwidth, and Q of Antennas," *IEEE transaction on Antennas and Propagation*, vol. 53, no. 4, pp. 1298-1324, April 2005.
- [4] J. S. McLean, "A re-examination of the fundamental limits on the radiation Q of electrically small antennas," *IEEE Transactions on Antennas and Propagation*, vol. 44, no. 5, pp. 672-676, May 1996.
- [5] Yamada, Y.; Michishita, N., "Antenna efficiency improvement of a miniaturized meander line antenna by loading a high ϵ_r dielectric material," *Antenna Technology: Small Antennas and Novel Metamaterials, 2005. IWAT 2005. IEEE International Workshop on*, vol., no., pp. 159- 162, 7-9 March 2005
- [6] Lin, C.-C.; Kuo, S.-W.; Chuang, H.-R.; , "A 2.4-GHz printed meander-line antenna for USB WLAN with notebook-PC housing," *Microwave and Wireless Components Letters, IEEE*, vol.15, no.9, pp. 546- 548, Sept. 2005
- [7] Jais, M.I.; Jamlos, M.F.; Malek, M.F.; Jusoh, M.; Adam, I.; Iliyes, N.I.; Saad, P.; , "Design Analysis of 2.45 GHz Meander Line Antenna (MLA)," *Intelligent Systems, Modelling and Simulation (ISMS), 2012 Third International Conference on*, vol., no., pp.628-631, 8-10 Feb. 2012
- [8] Y. Cho, S. Hwang and S. Park, "Printed antenna with folded non-uniform meander line for 2.4/5 GHz WLAN bands," *Electronics Letters*, vol. 41, no. 14, pp. 786 - 788 , 7 July 2005.
- [9] Li Jian-ying; Yu YuKy; GanYeowBeng; , "Analysis of Dual-Band Meander Line Antenna," *Antennas and Propagation Society International Symposium 2006, IEEE*, vol., no., pp.2033-2036, 9-14 July 2006
- [10] Khaleghi, A.; , "Dual Band Meander Line Antenna for Wireless LAN Communication," *Antennas and Propagation, IEEE Transactions on*, vol.55, no.3, pp.1004-1009, March 2007
- [11] Jamil, A.; Yusoff, M.Z.; Yahya, N., "An electrically small meander line antenna for wireless applications," *Circuits and Systems (APCCAS), 2010 IEEE Asia Pacific Conference on*, vol., no., pp.72-75, 6-9 Dec. 2010
- [12] J. Jung, H. Lee and Y. Lim, "Broadband flexible meander line antenna with vertical lines," *Microwave and Optical Technology Letters*, vol. 49, no. 8, pp. 1984-9187, August 2007.
- [13] D. Misan, I. A. Salamat, M. F. A. Kadir, M. R. C. Rose, M. S. R. M. Shah, M. Z. A. A. Aziz, M. N. Husain and P. Soh, "The study of meander line for microstrip and planar design," in *8th international conference on ITS telecommunications*,

- Phuket, 2008.
- [14] C. Veyres and V. F. Hanna, "Extension of the application of conformal mapping techniques to coplanar lines with finite dimensions," *International Journal of Electronics*, vol. 48, no. 2, pp. 47-56, 17 December 1979.
- [15] W. Hilberg, "From Approximations to Exact Relations for Characteristic Impedances," *IEEE Transactions on Microwave Theory and Techniques*, vol. 17, no. 5, pp. 259-265, May 1969.
- [16] G. Ghione, "Analytical formulas for coplanar lines in hybrid and monolithic MICs," *IEEE Electronics Letters*, vol. 20, no. 4, pp. 179-181, 16 February 1984.
- [17] F. T. Ulaby, "Chapter 2 Transmission Lines," in *Fundamentals of Applied Electromagnetics*, Fifth, Ed., Upper Saddle River, New Jersey: Pearson Prentice Hall, 2007, pp. 40-100.
- [18] C. A. Balanis, "Chapter 4 Linear Wire Antennas," in *Antenna Theory Analysis and Design*, Third ed., Hoboken, New Jersey: John Wiley & Sons, Inc., 2005, pp. 151-219.